

University of Missouri, St. Louis

IRL @ UMSL

Theses

UMSL Graduate Works

5-14-2020

The Primary Volatile Composition of Comet C/2015 ER61 (PANSTARRS)

Aaron Butler

University of Missouri-St. Louis, awbr4d@umsl.edu

Follow this and additional works at: <https://irl.umsl.edu/thesis>



Part of the [Atomic, Molecular and Optical Physics Commons](#), [Optics Commons](#), and the [Statistical Models Commons](#)

Recommended Citation

Butler, Aaron, "The Primary Volatile Composition of Comet C/2015 ER61 (PANSTARRS)" (2020). *Theses*. 385.

<https://irl.umsl.edu/thesis/385>

This Thesis is brought to you for free and open access by the UMSL Graduate Works at IRL @ UMSL. It has been accepted for inclusion in Theses by an authorized administrator of IRL @ UMSL. For more information, please contact marvinh@umsl.edu.

The Primary Volatile Composition of Comet C/2015 ER61 (PANSTARRS)

by

Aaron Wayne Butler

B.S. Physics, University of Missouri-St. Louis, 2016

A Thesis

Submitted to The Graduate School of the

University of Missouri-St. Louis

In partial fulfillment of the requirements of the degree

Master of Science

In

Physics

May 2020

Advisory Committee

Erika Gibb Ph. D.

Bruce Wilking Ph. D.

Sonya Bahar Ph. D.

Abstract

In the outer edges of the solar system exist two regions: the Kuiper belt and Oort cloud. These two regions have a high amount of icy bodies (comets) orbiting the Sun. Comets located within the Oort cloud and Kuiper belt contain an ancient codex to the solar systems contents, before the formation of our solar system. Presented are near-infrared, high-resolution ($\lambda/\Delta\lambda \sim 40000$) data obtained from the immersion-grating echelle spectrograph iSHELL at the 3m NASA Infrared Telescope Facility (IRTF) in Maunakea, Hawaii of the Oort cloud comet C/2015 ER61 (PANSTARRS). Observations took place on April 15 and 17 in 2017 while the comet was declining after a dramatic outburst. We used two settings (LCustom and LP1) to measure the production rates and abundances (or upper limits) of H₂O, CH₃OH, C₂H₂, C₂H₆, HCN, and H₂CO. We found the comet to be enriched in C₂H₂, normal in H₂CO, and depleted in other detected volatiles compared to other Oort cloud comets.

1. Introduction

The solar system as we know it today with planets, asteroids, moons, and comets is very different from how it was ~ 4.6 billion years ago. The proto star that became our Sun was surrounded by matter that moved in the shape of a disc. The disc that surrounds a proto-star is called a proto-planetary disc. It is believed that the materials that formed comets surrounding the solar system existed near the midplane of the proto-planetary disc at a distance greater than 5 AU (Mumma and Charnley 2011) where the temperatures were low enough for ices to condense. A few AU away from the proto-star, materials in the middle of the plane are significantly cooler and are protected from the radiation emitted from the proto star. As the proto star develops into a star on the main sequence, the radiative pressure pushes lighter material further out. During this time the planets formed from the left-over rocky material and icy masses of gas/water. This chaotic period of colliding bodies is called the heavy bombardment. Comets during the late heavy bombardment may have played a pivotal role in delivering water and other volatiles needed for Earth's oceans and to allow life to form on Earth. During this transitional period as the planets formed, a majority of comets were gravitationally scattered by the larger Jovian planets and were deposited in two reservoirs. These two reservoirs are called the Oort cloud (hereafter OC) and the Kuiper belt (Gladman 2005, Mumma and Charnley 2011).

Comets within the OC have remained relatively untouched by events that happened over ~ 4.6 billion years since our Sun formed. Therefore, comets contain one of the most pristine records of pre-solar times and early transitional times. Most interactions considered to alter the nucleus during its time in the OC or Kuiper belt are expected to affect only a thin layer (a few meters deep). This layer is shed as the comet makes its way into the inner solar system (Stern

2003). Over the past ~30 years astronomers have been observing comets with near-infrared spectroscopy in order to ascertain what volatiles these bodies contain. In the near-infrared, comet spectra are rich in rovibrational emission lines due to water and simple organic molecules. These molecules are excited by solar photons and then emit photons from these excited rovibrational levels that can be seen through Earth's atmosphere (Dello Russo et al. 2004).

Comets are important tools for studying the solar system's past. Measuring materials contained within these bodies gives us a look at the primitive makeup of our solar system and possibly where many of Earth's volatiles came from like H₂O and HDO. Currently, there are many studies attempting to classify and model previous comets with new ones being added when observed. The classification and taxonomies of these icy bodies is ongoing. Early studies suggested three taxonomic classes: "organics-normal", "organics-enriched", or "organics depleted" (Mumma and Charnley 2011 and references therein). These classifications are based upon the ratios of the primary volatiles (CO, H₂CO, CH₃OH, CH₄, C₂H₂, C₂H₆, HCN, NH₃, and OCS) to that of H₂O (the most abundant volatile in comets). However, recent studies show that many comets do not fit into any of the proposed classifications (Roth et al. 2018; DiSanti 2017). These emergent studies challenge the current classification system (Gibb et al. 2012; Mumma and Charnley 2011).

Comet C/2015 ER61 (PANSTARRS) was discovered by the Pan-STARRS1 telescope on Haleakala on March 14, 2015. It has a highly eccentric orbit (an extremely elongated orbit) and a far distant aphelion (furthest distance in an objects orbit) ($e = 0.9973$, $a = 385$ au) which suggests an origin in the inner OC (Meech et al. 2017). During its discovery, Comet C/2015 ER61 (PANSTARRS) appeared asteroidal without a visible coma detected. At first it was thought to be

a Manx comet, which is an observationally inactive or nearly inactive object from the OC (Meech et al. 2017). A few months after its initial discovery the comet became visually active. A faint coma was detected by the Gemini telescope in June 2015 when the comet was 7.7 AU from the sun. On April 4, 2017 Comet C/2015 ER61 (PANSTARRS) began to outburst with a visual magnitude of 6.2 (Yang et al 2017). The outburst provided us the opportunity on our observation dates to study materials that are exposed from deeper within the comet by the outburst. The materials deep within the comet are protected from surface interactions caused by space weathering and cometary activity. The outburst also allowed us to view the comet at a higher visual magnitude. As we began to observe C/2015 ER61 (PANSTARRS) ten days after the outburst. Keeping the taxonomic classification in mind, we add the volatile composition of C/2015 ER61 (PanSTARRS) to the list of observed comets. In section 2 we discuss the observations and data analysis. In section 3 we present the results. In section 4, we discuss our results and compare them to other comets that have been observed.

2. Observations and Data Reduction

During its 2017 apparition comet C/2015 ER61 (PanSTARRS) (hereafter ER61) was closest to Earth (1.2 au) on April 19, 2017 and reached perihelion on May 10, 2017. We observed ER61 with the 3m telescope at NASA IRTF at Maunakea, HI using the high-resolution ($\lambda/\Delta\lambda\sim 40000$), near-infrared, immersion-grating echelle spectrograph iSHELL in order to measure its volatile composition (Rayner et al. 2016). In order to gather a large suite of molecular abundances we chose iSHELL settings (LP1 and LCustom) focusing on L-band emission using a 3.6 μm narrow band filter. We also defined cross-disperser positions (specifically L-Custom setting) in order to measure H_2O simultaneously with minor species (NH_3 , HCN and C_2H_2) in the 3 μm region. The observations discussed in this paper took place on April 15th and 17th of 2017 (see Table 1).

Observations were performed with a 6-pixel (0."75) wide slit, using a standard ABBA nod pattern, with A and B beams symmetrically placed about the midpoint along the 15" long slit and separated by half its length. Combining spectra of the noded beams as (A–B)–(B–A) cancelled emissions from thermal background, instrumental biases, and "sky" emission (lines and continuum) to second order in air mass. The telescope could not maintain guiding on both dates, so we manually registered the A and B beams to put the comet in the same row for each frame so that the exposures could be combined. The data were flat-fielded, dark subtracted, and cleaned of hot pixels and cosmic ray strikes. A flux calibration was performed using appropriately placed bright standard stars on each date using a wide (4."0) slit. Our data reduction procedures are described in the peer reviewed literature (Bonev 2005; Disanti et al. 2006, 2014; Radeva et al. 2010; Villanueva et al. 2009) Further elaboration on special aspects of iSHELL spectra reduction is detailed in Sec. 3.2 of Disanti et al. (2017).

We determined contributions from atmospheric emission/absorption and emission from ER61 spectra as described previously in Disanti et al. (2017). We synthesized atmospheric spectra using the Line-By-Line Spectral Transmittance Model optimized for Maunakea's atmospheric conditions (Clough et al. 2005). These models were used to account for the atmosphere between the telescope and ER61 by retrieving column burdens for atmospheric absorption. The models were sampled to the resolution of the data and then normalized to the comet's continuum level. By subtracting the atmospheric models from the extracted cometary spectra, we were able to detect emission lines from ER61. Growth factors, defined as $GF = Q_{\text{global}}/Q_{\text{NC}}$, where Q_{NC} is the nucleo-centric production rate, were determined for both the gas and the dust when there was sufficient signal-to-noise. This is done because the nucleus centered position has losses due to seeing and telescope tracking. Production rates ($Q_{\text{(molecule)}} \text{ s}^{-1}$) were determined using the Q-curve methodology (Bonev 2005; Gibb et al. 2012) which considers emission intensity on either side of the nucleus. We assume a spherical symmetric outflow velocity of 0.8 km/s at 1 AU (scaled as heliocentric distance $v_{\text{gas}} = 0.8 R_{\text{helio}}^{-0.5}$ km/s) as outlined in Section 3.2.2 of Disanti et al. (2016)

Table 1

Observing Log and H₂O Production Rates

UT Date	IShell Setting	UT	R_h	dR_h/dt	Δ	$d\Delta/dt$	T_{int}	$Q(\text{H}_2\text{O})$
			(AU)	(km s ⁻¹)	(AU)	(km s ⁻¹)	(minutes)	(10 ²⁹ s ⁻¹)
2017 April 15	Lp1	15:29-15:58	1.118	-10.40	1.180	-2.31	29	*
2017 April 17	LCustom	15:01-15:47	1.107	-9.677	1.178	-1.22	43	1.15

Notes. R_h , dR_h/dt , Δ , and $d\Delta/dt$ are heliocentric distance, heliocentric velocity, geocentric distance, and velocity towards the observer, respectively, of ER61; T_{int} is total integration time on ER61, and $Q(\text{H}_2\text{O})$ is the water production rate.

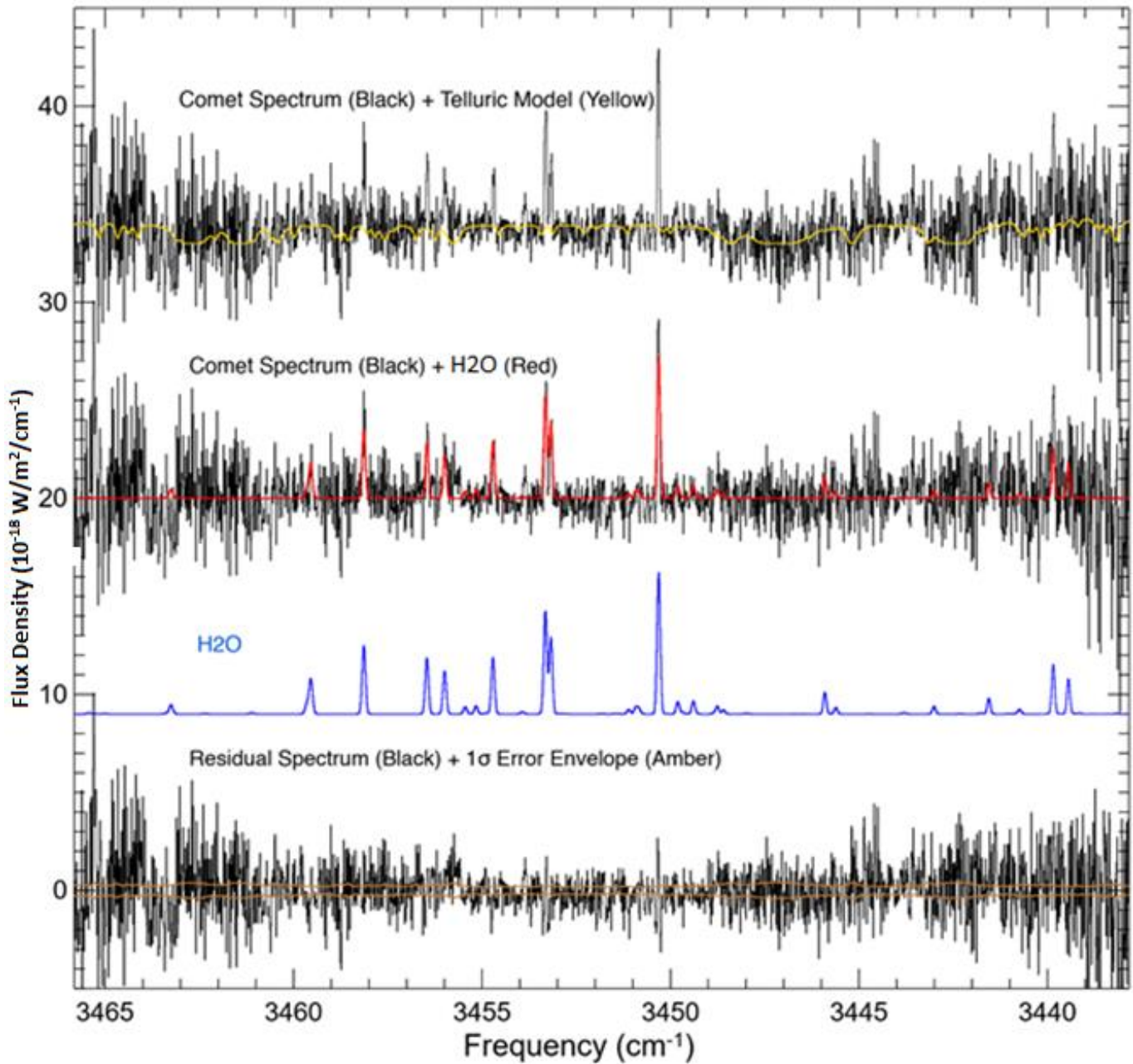
3. Results

We were able to detect fluorescent emission from H₂O, CH₃OH, C₂H₂, C₂H₆, HCN, and H₂CO. After correcting for the monochromatic atmospheric transmittance at its Doppler-shifted wavelength (according to the velocity of the comet towards Earth at the time of observation), synthetic models of fluorescent emission for each targeted molecule were compared to observed emission line intensities. We obtained a rotational temperature using correlation and excitation analysis as discussed in Bonev et al. (2008). After running rotational temperature extraction for each individual molecule, we found that H₂O was the best constrained. The best constrained order for water was Order 179 obtained on April 17, 2017. On April 15, 2017, a rotational temperature could not be narrowed down satisfactorily due to lack of strong H₂O lines within the orders sampled. H₂O is favored for obtaining a rotational temperature because the emission lines span a broad range of excitation energies and are intrinsically bright. Instead of using a rotational temperature that is not well constrained on April 15, we adopted the rotational temperature obtained on April 17. Previous observations of other comets show that the rotational temperature is often consistent over a span of days at this heliocentric distance. We could not detect CH₄ because of the low relative velocity of ER61 towards us. A doppler shift >10km/s would be best to detect CH₄ in order to distinguish the emission lines from those of Earth's atmosphere.

“Best-fit” spectra and models are shown for Order 179 in Figure 1. Models for HCN and Order 155 (C₂H₆, OH, CH₃OH) are also shown in Figures 2 and 3, respectively. Due to low signal-to-noise for Order 171, we were only able to detect HCN with a high degree of certainty. We

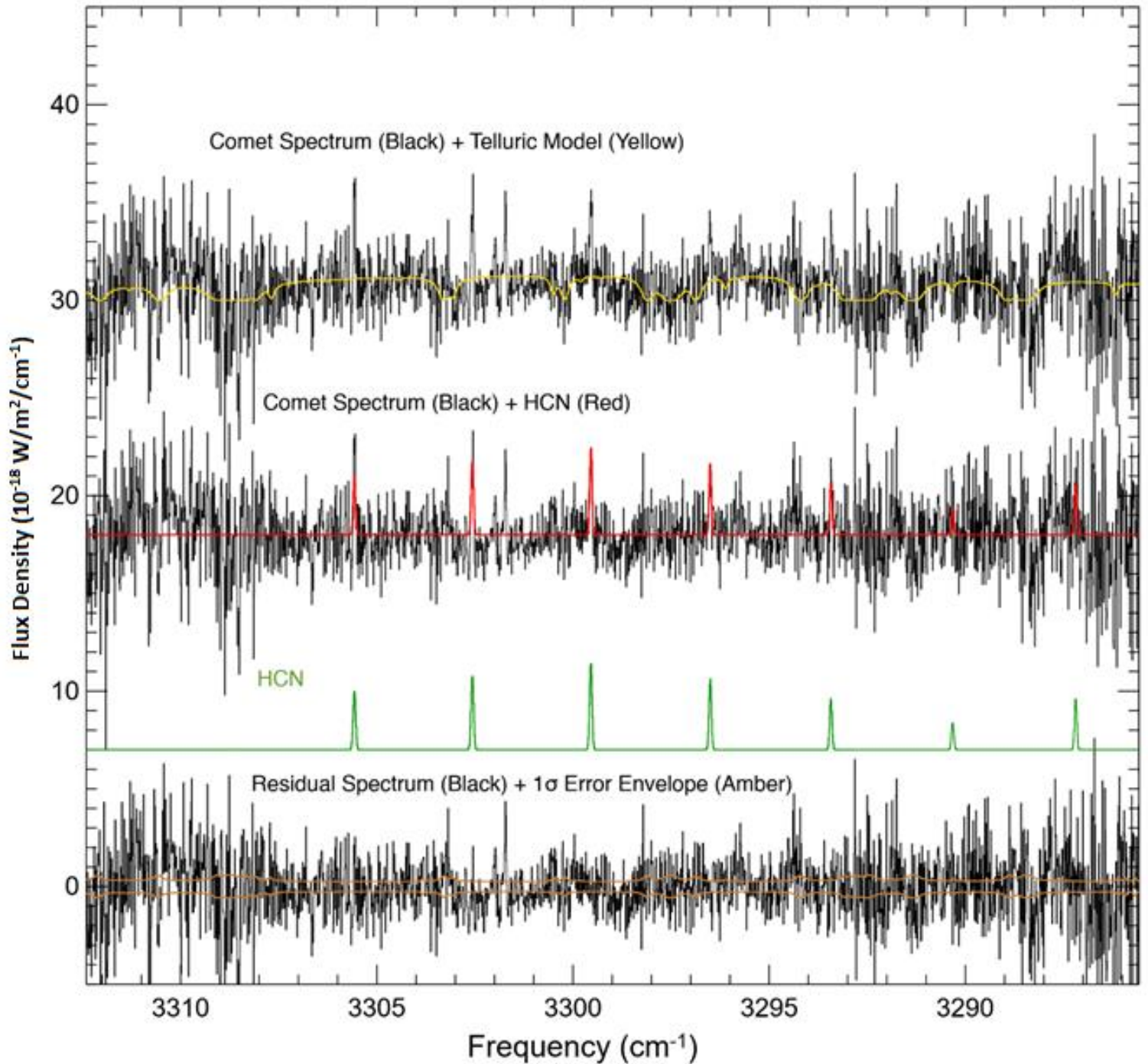
report upper limits for NH_3 and OH on that day. Growth factors, best-fit rotational temperatures, production rates, and mixing ratios for each date are shown in Table 2.

Figure 1



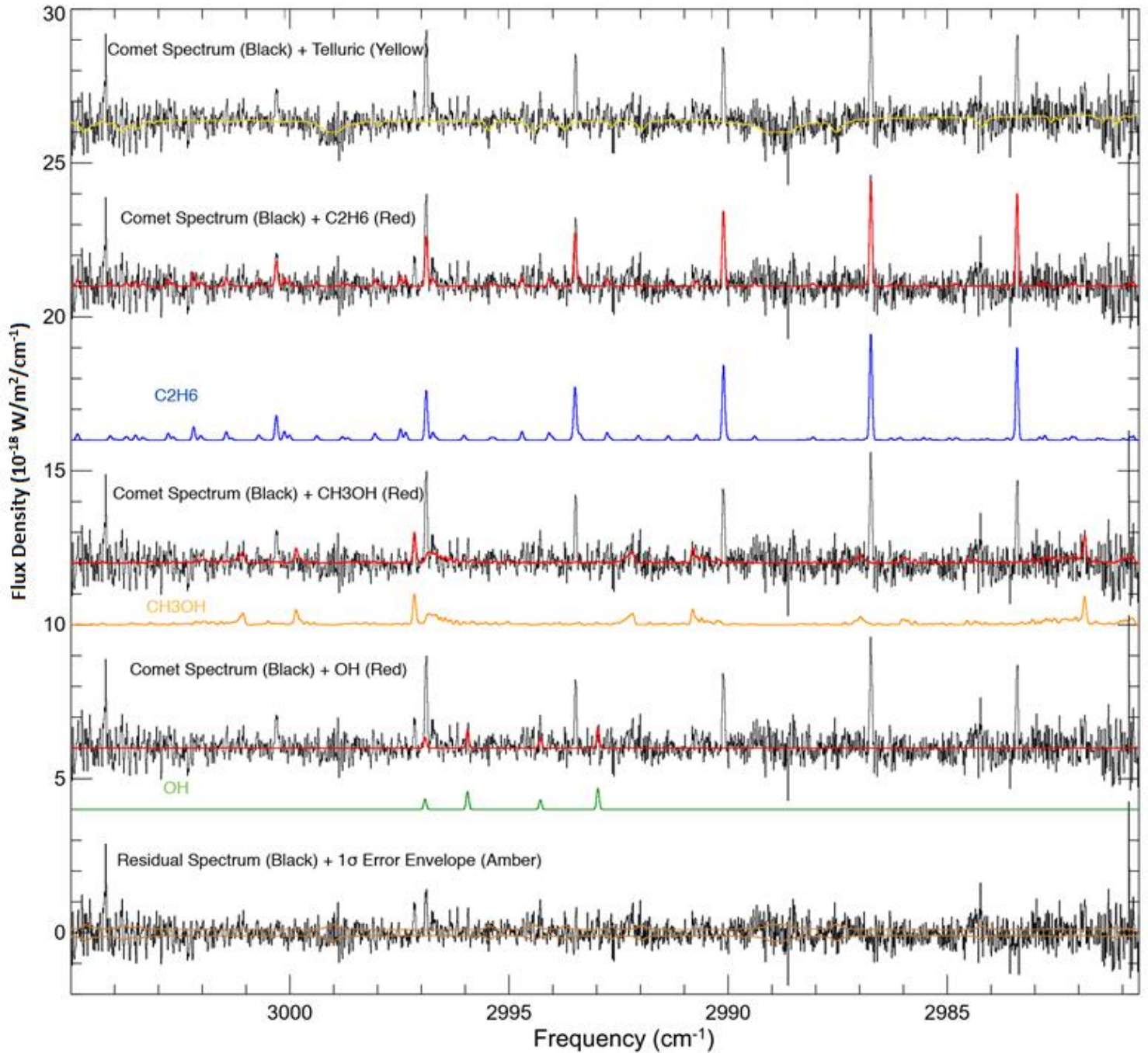
Notes - Detection of H₂O in comet C/2015 ER61 from Order 179 on April 17, 2017. The comet spectrum (after subtracting the telluric model) is plotted in black with the yellow telluric model plotted over that. Below is the best fit fluorescent emission model for H₂O in red overlaid onto the comet spectrum (black). In blue is the H₂O emission model offset for clarity. The residual (spectrum – model, black) and 1σ error envelopes (amber) are plotted at the bottom of each panel

Figure 2



Notes - Detection of HCN in comet C/2015 ER61 from Order 171 on April 17, 2017. The comet spectrum (after subtracting the telluric model) is plotted in black with the yellow telluric model plotted over that. Below is the individual best fit fluorescent emission model for HCN in red overlaid onto the comet spectrum (black). In green is the HCN emission model offset for clarity. The residual (spectrum – model, black) and 1σ error envelopes (amber) are plotted at the bottom of each panel.

Figure 3



Notes - Detection suite of C_2H_6 , CH_3OH , and OH in comet C/2015 ER61 from Order 155 on April 15, 2017. The comet spectrum (after subtracting the telluric model) is plotted in black for C_2H_6 , CH_3OH , and OH respectively in red overlaid onto the comet spectrum (black). In blue is the C_2H_6 emission model offset for clarity. In orange is CH_3OH emission model offset for clarity. In green is OH emission model offset for clarity. The residual (spectrum - model, black) and 1σ error envelopes (amber) are plotted at the bottom of the panel.

Table 2

iSHELL Setting	Molecule	$T_{\text{rot}}^{\text{a}}$ (K)	Growth Factor	Q^{e} $10^{27} \text{ mol s}^{-1}$	$Q_{\text{x}}/Q(\text{H}_2\text{O})^{\text{b}}$ (%)
April 15, $R_{\text{h}} = 1.119 \text{ AU}$, $\Delta = 1.180 \text{ AU}$					
Lp1	C ₂ H ₆	(67)	1.46 ± 0.07	0.441 ± 0.038	0.374 ± 0.01
	CH ₃ OH	(67)	1.47	1.37 ± 0.34	1.16 ± 0.08
	CH ₃ OH	(67)	(1.46) ^d	1.44 ± 0.19	1.25 ± 0.03
	H ₂ CO	(67)	2.91 ± 0.26	0.41 ± 0.18	0.35 ± 0.12
	OH	(67)	1.46	440 ± 182	*
April 17, $R_{\text{h}} = 1.107 \text{ AU}$, $\Delta = 1.179 \text{ AU}$					
LCustom	H ₂ O	67^{+9}_{-7}	2.11 ± 0.32	115 ± 13.1	100
	H ₂ O*	(67)	1.95 ± 0.40	98 ± 6.49	*
	OH	67	(2.11) ^d	397 ± 148	*
	HCN	(67)	2.07 ± 0.25	0.152 ± 0.025	0.144 ± 0.01
	NH ₃ ^c	(67)	(2.07) ^d	< 0.20	< 0.17
	C ₂ H ₂	(67)	(2.07) ^d	0.21 ± 0.06	0.17 ± 0.04

Notes

^a Rotational temperature. Values in parentheses are assumed from T_{rot} water on April 17, 2017

^b Production rate ratio per molecule compared to water value

^c Values from NH₃ are 3σ upper limits

^d Assumed growth factor

^e Production rate errors include line-by-line deviation between the model and observed intensities in photon noise. (Bonev 2005; Dello Russo et al. 2004; Bonev et al. 2007)

^f CH₃OH production rate from Lp1 order 155

^g H₂O production rate from LCcustom order 181

4. Discussion

The outbursting of ER61 was a very lucky occurrence. Since ER61 exhibited behavior like a Manx comet, the intrinsic brightness of it was very low. Data from later dates in May 2017 reveal a hard to see continuum due to the fading brightness. Classifying ER61 is very difficult indeed as outlined under the system in Mumma and Charnley (2011). A study conducted by Dello Russo et al. (2016) and references therein reveal how different Oort cloud comets can be when compared.

Given that there are some 10^{11} comets in the OC around our solar system, the sample size of comets characterized in the near-infrared is very small (~30 Oort cloud Comets) (Emel'Yanenko et al. 2007). Using available data from other OC comets we have compiled a cometary median of volatile ratios to that of water for each volatile found in ER61 for comparison which we present in Table 3. We find ER61 to be depleted in HCN, C₂H₆, CH₃OH, and NH₃ (given the upper limit for NH₃). ER61 is consistent with the mean for H₂CO and C₂H₂ despite uncertainties in signal to noise. The abundances found in ER61 are very similar to those of C/2012 S1 (Dello Russo et al. 2016) another OC family comet.

There is also compelling evidence that ER61 underwent a nucleus splitting event during the outburst. The detection of a secondary nucleus occurred on June 11, 2017. The secondary piece of ER61 had a variable brightness that fluctuated by three orders of magnitude compared to the primary nucleus of ER61 (Zdenek 2016). The Zdenek paper has yet to be published in a refereed journal but offers a compelling possibility that other papers on the secondary nucleus of ER61 yet to be published could be in the works. If other studies on the secondary nucleus are

published it would provide a chance to compare for heterogeneity in the nucleus of ER61. Only time will tell if other studies have taken place on the possible secondary nucleus.

ER61 reached perihelion on May 10. Preliminary results from observations in May 2017 of ER61 offer us a chance for comparison (Saki, personal communication) pre- and post-perihelion. Water production rates from May 11, 2017 and May 13, 2017 are diminished which is to be expected as the nucleus moves further away from the Sun. ($7.22 \times 10^{28} \text{ s}^{-1}$ on May 11 and $4.19 \times 10^{28} \text{ s}^{-1}$ on May 13 compared to $1.15 \times 10^{29} \text{ s}^{-1}$). The T_{rot} from the May observations was measured at 60 Kelvin. Mixing ratios of volatiles compared to water from the May observation show depletion in NH_3 , C_2H_6 , and HCN which is consistent with results from April. Preliminary results also show enrichment in C_2H_2 and possible enrichment in CH_3OH (might be issues with signal-to-noise, results show a big swing in error $\sim 0.75\%$). C_2H_2 enrichment is consistent with results from April, however results from April show a depletion in CH_3OH . Results for H_2CO were better constrained than the April dates and appear to be normal compared to other OC comets.

The current taxonomic system used to classify comets as “organics-normal”, “organics-depleted”, or “organics-enriched” is too simple of a classification system given the dynamic variability of the comets studied. As more observations take place and more sensitive instruments are developed and installed on telescopes like iSHELL on NASA’s Infrared Telescope Facility, we will have a better answer for the volatile abundances within comets and the possibility of a more dynamic classification system. A more robust classification system in combination with protoplanetary disc models, could eventually help us to understand how volatiles were formed and distributed in the early solar system.

Table 3

Molecule	Abundance in ER61 ^a	Median Abundance in OC Comets ^b
C ₂ H ₂	0.17%	0.13%
C ₂ H ₆	0.37%	0.65%
CH ₃ OH	1.16%	2.16%
H ₂ CO	0.35%	0.32%
HCN	0.14%	0.26%
NH ₃	<0.20%	0.94%

Notes

^a Abundances are given as an average if possible for both dates.

^b Cometary median abundances calculated from abundances in OC comets in 8p/Tuttle (Bonhardt et al. 2008), 153P/I-Z (Biver et al. 2006), C/1995 O1 (Biver et al. 2002; Dello Russo et al. 2000; Dello Russo et al. 2001; Magee-Sauer et al. 1999), C/1996 B2 (Mumma et al. 1996; Magee-Sauer et al. 2002), C/1999 H1 (Mumma et al. 2001; Dello Russo et al. 2006), C/1999 S4 (Bockelée-Morvan et al. 2001), C/1999 T1 (Biver et al. 2006; Schleicher et al. 2001), C/2000 WM1 (Radeva et al. 2010; Biver et al. 2006), C/2001 A2 (Gibb et al. 2007), C/2002 T7 (Hogerheijde et al. 2009; DiSanti et al. 2006), C/2003 K4 (Paganini et al. 2015), C/2004 Q2 (Kobayashi et al. 2009), C/2006 M4 (DiSanti et al. 2009), C/2006 P1 (Dello Russo et al. 2009), C/2007 N3 (Gibb et al. 2012), C/2007 W1 (Villanueva et al. 2011), C/2009 P1 (Gicquel et al. 2015), C/2010 G2 (Kawakita et al. 2014), C/2012 F6 (Paganini et al. 2014a; Biver et al. 2014), C/2013 R1 (Paganini et al. 2014b; Biver et al. 2014), C/2012 S1 (Dello Russo et al. 2016)

5. Acknowledgements

Data presented and discussed in this paper were obtained by the visiting astronomer at the Infrared Telescope Facility, which is operated by the University of Hawaii under contract NNH14CK55B with the National Aeronautics and Space Administration. I wish to recognize and acknowledge the very significant cultural role and reverence that the summit of Maunakea has always had within the indigenous Hawaiian community. We are most fortunate to have the opportunity to conduct observations from this mountain.

6. References

- Biver, N., Bockelée-Morvan, D., Crovisier, J., et al., 2006. Radio wavelength molecular observations of comets C/1999 T1 (McNaught-Hartley), C/2001 A2 (LINEAR), C/2000 WM1 (LINEAR) and 153P/Ikeya–Zhang, *Astronomy and Astrophysics* 449, 1255–1270
- Biver, N., Bockelée-Morvan, D., Colom, P., et al., 2002. The 1995 – 2002 long-term monitoring of comet C/1995 O1 (Hale–Bopp) at radio wavelengths, *Earth, Moon Planets* 90, 5–14
- Biver, N., Bockelée-Morvan, D., Debout, V., et al., 2014. Complex organic molecules in comets C/2012 F6 (Lemmon) and C/2013 R1 (Lovejoy): Detection of ethylene glycol and formamide, *Astronomy and Astrophysics* 566, 5
- Bonev, B. P., 2005. Towards a Chemical Taxonomy of Comets: Infrared Spectroscopic Methods for Quantitative Measurements of Cometary Water (With an Independent Chapter on Mars Polar Science), PhD thesis, University of Toledo
- Bonev, B.P., Mumma, M.J., Radeva Y.L., et al. 2008. The Peculiar Volatile Composition of Comet 8P/Tuttle: A Contact Binary of Chemically Distinct Cometesimals?, *Astrophysical Journal Letters* 680, L61
- Bohnhardt, H., Mumma, M.J., Villanueva, G.L., et al., 2008. The unusual volatile composition of the Halley-type comet 8P/Tuttle: Addressing the existence of an inner Oort cloud, *Astrophysical Journal* 683, L71–L74

- Bockelée-Morvan, D., Biver, N., Moreno, R., et al., 2001. Outgassing behavior and composition of comet C/1999 S4 (LINEAR) during its disruption, *Science* 292, 1339–1343
- Clough, S.A., Shephard, M.W., Mlawer, E.J., Delamere, J.S., Iacono, M.J., Cady-Pereira, K. et al., 2005. Atmospheric radiative transfer modeling: a summary of the AER codes, *Journal of Quantitative Spectroscopy and Radiative Transfer* 91, 233
- DiSanti, M.A. Bonev, B.P., Dello Russo, N. Vervack Jr., R.J., Gibb, E.L., Roth, N.X., McKay, A.J., Kawakita, H., Feaga, L.M., Weave, H.A., 2017. Hypervolatiles in a Jupiter-family Comet: Observations of 45P/Honda-Mrkos-Pajdušáková Using iSHELL at the NASA-IRTF, *Astronomical Journal* 154, 246
- DiSanti, M.A., Villanueva, G.L., Milam, S.N., et al., 2009. A multi-wavelength study of parent volatile abundances in Comet C/2006 M4 (SWAN), *Icarus* 203, 589–598
- DiSanti, M. A., Bonev, B. P., Magee-Sauer, K., Russo, D., Mumma, M.J., Reuter, D.C., Villanueva, G.L., 2006. Detection of Formaldehyde Emission in Comet C/2002 T7 (LINEAR) at Infrared Wavelengths: Line-by-Line Validation of Modeled Fluorescent Intensities, *Astrophysical Journal* 650, 470
- DiSanti, M. A., Villanueva, G. L., Paganini, L., Bonev, B.P., Keane, J.V., Meech, K.J. Mumma, M.J., 2014, Volatile Composition of Comets: Emphasis on Oxidized Carbon, *Icarus* 228, 167
- Dello Russo, N., Mumma, M.J., DiSanti, M.A., et al., 2000. Water production and release in comet C/1995 O1 Hale–Bopp, *Icarus* 143, 324–337

- Dello Russo, N., Mumma, M.J., DiSanti, M.A., et al., 2001. Ethane production and release in Comet C/1995 O1 Hale–Bopp, *Icarus* 153, 162–179
- Dello Russo, N., Mumma, M.J., DiSanti, M.A., et al., 2006. A high-resolution infrared spectral survey of comet C/1999 H1 Lee, *Icarus* 184, 255–276
- Dello Russo, N., DiSanti, M.A., Magee-Sauer, K., Gibb, E.L., Mumma, M.J., Barber, R.J., & Tennyson, J., 2004. Water production and release in Comet 153P/Ikeya-Zhang (C/2002 C1): Accurate rotational temperature retrievals from hot-band lines near 2.9- μm , *Icarus* 168, 186-200
- Dello Russo, N., Vervack, R.J., Weaver, H.A., et al., 2009b. Infrared measurements of the chemical composition of C/2006 P1 McNaught, *Icarus* 200, 271–279
- Dello Russo, N., Vervack, R.J., Kawakita Jr., H., et al., 2016. The compositional evolution of C/2012 S1 (ISON) from ground-based high-resolution infrared spectroscopy as part of a worldwide observing campaign, *Icarus* 266, 152–172
- Dello Russo, N., Kawakita, H., et al. 2016. Emerging trends and a comet taxonomy based on the volatile chemistry measured in thirty comets with high-resolution infrared spectroscopy between 1997 and 2013, *Icarus* 278, 301–332
- Gibb, E.L., Mumma, M.J., Dello Russo, N., DiSanti, M.A., and Magee-Sauer, K. 2003. Methane in Oort cloud comets, *Icarus* 165, 391

- Gibb, E.L., DiSanti, M.A., Magee-Sauer, K., et al., 2007. The organic composition of C/2001 A2 (LINEAR) II. Search for heterogeneity within a comet nucleus, *Icarus* 188, 224–232
- Gibb, E.L., Bonev, B.P., Villanueva, G.L., et al., 2012. Chemical composition of comet C/2007 N3 (Lulin): Another “atypical” comet, *Astrophysical Journal* 750 (102), 14
- Gicquel, A., Milam, S., Cordiner, M., et al., 2015. The evolution of volatile production in comet C/2009 P1 (Garradd) during its 2011–2012 apparition, *Astrophysics Journal* 807, 19
- Gladman, B. 2005. The Kuiper belt and the Solar System's Comet Disk, *Science* 307, 71
- Hogerheijde, M.R., Qi, C., de Pater, I., et al., 2009. Simultaneous observations of comet C/2002 T7 (LINEAR) with the Berkeley-Illinois-Maryland association and Owens Valley radio observatory. Interferometers: HCN and CH₃OH, *Astronomy Journal* 137, 487–4845
- Kawakita, H., Dello Russo, N., Vervack Jr., R.J., et al., 2014. Extremely organic-rich coma of comet C/2010 G2 (Hill) during its outburst in 2012, *Astrophysics Journal* 788 (110), 7.
- Kobayashi, H., Kawakita, H., 2009. Formation conditions of icy materials in comet C/2004 Q2 (Machholz). I. Mixing ratios of organic volatiles, *Astrophysics Journal* 703, 121–130
- Magee-Sauer, K., Mumma, M.J., DiSanti, M.A., et al., 1999. Infrared spectroscopy of the v₃ band of hydrogen cyanide in C/1995 O1 Hale–Bopp, *Icarus* 142, 498–508

- Magee-Sauer, K., Mumma, M.J., DiSanti, M.A., et al., 2002. Hydrogen cyanide in comet C/1996 B2 Hyakutake, *Geophysical Research* 107 (E11), 5096.
- Meech, K.J., Schambeau, C.A., Sorli, K., Kleyna, J.T., Micheli, M., James, B., Denneau, L., Keane, J.V. Toller, E. Wainscoat, R., 2017. Beginning of activity in long-period comet C/2015 ER61 (PANSTARRS), *The Astronomical Journal* 153, 206
- Mumma, M.J., DiSanti, M.A., Dello Russo, N., et al., 1996. Detection of Abundant Ethane and Methane, Along with Carbon Monoxide and Water, in Comet C/1996 B2 Hyakutake: Evidence for Interstellar Origin, *Science* 272, 1310–1314
- Mumma, M.J., McLean, I.S., DiSanti, M.A., et al., 2001a. A survey of organic volatile species in comet C/1999 H1 (Lee) using NIRSPEC at the Keck observatory, *Astrophysics Journal* 546, 1183–1193
- Mumma, M.J. and Charnley, S.B. 2011. The Chemical Composition of Comets—Emerging Taxonomies and Natal Heritage, *The Annual Review of Astronomy and Astrophysics* 49, 471
- Paganini, L., Mumma, M.J., Villanueva, G.L., et al., 2015. The volatile composition of comet C/2003 K4 (LINEAR) at near-IR wavelengths – Comparisons with results from the Nancay radio telescope and from the Odin, Spitzer, and SOHO Space observatories, *Astrophysics Journal* 808 (1), 8
- Paganini, L., DiSanti, M.A., Mumma, M.J., et al., 2014a. The unexpectedly bright comet C/2012 F6 (Lemmon) unveiled at near-infrared wavelengths, *Astronomy Journal*, 147, 11

Paganini, L., Mumma, M.J., Villanueva, G.L., et al., 2014b. C/2013 R1 (Lovejoy) at IR wavelengths and the variability of CO abundances among Oort cloud comets, *Astrophysics Journal* 791 (122), 8

Radeva, Y.L., Mumma, M.J., Bonev, B.P., et al., 2010. The organic composition of comet C/2000 WM1 (LINEAR) revealed through infrared spectroscopy, *Icarus* 206, 764–777

Roth, N.X., Gibb, E.L., Bonev, B.P., DiSanti, M.A., Dello Russo, N., Vervack, R.J., McKay, A.J., Kawakita, H., 2018. A Tale of “Two” Comets: The Primary Volatile Composition of Comet 2P/Encke Across Apparitions and Implications for Cometary Science, *Astronomical Journal* 156, 6

Schleicher, D. 2001. Comet C/1999 T1 (McNaught-Hartley), *Icarus* 2, 437

Stern, S. Alan 2003. The evolution of comets in the Oort cloud and Kuiper belt, *Nature* 424, 639

Villanueva, G. L., Mumma, M. J., Bonev, B. P., et al. 2009. A Sensitive Search for Deuterated Water in Comet 8P/TUTTLE, *Astrophysics Journal* 690, L5

Villanueva, G.L., Mumma, M.J., DiSanti, M.A., et al., 2011. The molecular composition of comet C/2007 W1 (Boattini): Evidence of a peculiar outgassing and a rich chemistry, *Icarus* 216, 227–240

Yang, B., Hustemakers, D., Shinnaka, S., Opitom, C., Manfroid, J., Jehin, E., Meech, K., Hainaut, O., Keane, J., 2017. Isotopic ratios in outbursting comet C/2015 ER61,

Astronomy and Astrophysics 609, 10